

PERFORMANCE ANALYSIS OF ORGANIC RANKINE CYCLES USING DIFFERENT WORKING FLUIDS

by

Qidi ZHU, Zhiqiang SUN^{*}, and Jiemin ZHOU

School of Energy Science and Engineering, Central South University, Changsha, China

Original scientific paper

DOI: 10.2298/TSCI120318014Z

Low-grade heat from renewable or waste energy sources can be effectively recovered to generate power by an organic Rankine cycle in which the working fluid has an important impact on its performance. The thermodynamic processes of organic Rankine cycles using different types of organic fluids were analyzed in this paper. The relationships between the organic Rankine cycle's performance parameters (including evaporation pressure, condensing pressure, outlet temperature of hot fluid, net power, thermal efficiency, exergy efficiency, total cycle irreversible loss, and total heat-recovery efficiency) and the critical temperatures of organic fluids were established based on the property of the hot fluid through the evaporator in a specific working condition, and then were verified at varied evaporation temperatures and inlet temperatures of the hot fluid. Here we find that the performance parameters vary monotonically with the critical temperatures of organic fluids. The values of the performance parameters of the ORC using wet fluids are distributed more dispersedly with the critical temperatures, compared with those of using dry/isentropic fluids. The inlet temperature of the hot fluid affects the relative distribution of the exergy efficiency, whereas the evaporation temperature only has an impact on the performance parameters using wet fluid.

Key words: organic Rankine cycle, low-grade heat recovery, organic working fluid, performance analysis

Introduction

The accelerated consumption of fossil fuels makes energy and environment related problems increasingly serious. Efficient utilization of low-grade heat from renewable or waste energy sources can save fuels and alleviate environmental pollution. The organic Rankine cycle (ORC) is an effective method for the recovery of low-grade heat to generate power. In an ORC the working fluid plays a pivotal role in the performance of the cycle, so appropriate selection of the working fluid is considered as the leading challenge in the ORC technology [1-3].

Studies on the performances of subcritical and supercritical ORC have been carried out for decades. Schuster *et al.* compared the supercritical ORC with the subcritical ones on the thermal efficiency, the system efficiency, and the exergy loss [4]. Guo *et al.* optimized the CO₂-based supercritical Rankine cycle and the R245fa-based subcritical ORC, and analyzed the natural and conventional working fluids-based transcritical Rankine power cycles driven by low-temperature geothermal sources [5, 6]. The effects of working fluids and conditions on the ORC performance were extensively examined. Liu *et al.* analyzed the effect of working fluids on the thermal efficiency and the total heat-recovery efficiency [7]. Wei *et al.* [8] studied the thermodynamic performance of the ORC using R245fa under disturbances [9].

* Corresponding author; e-mail: zqsun@csu.edu.cn

Etemoglu found the first and the second law efficiencies increased with the evaporation temperature for geothermal power generation systems. Tchanche *et al.* [10] deemed that R134a was the most suitable working fluid for small scale solar applications by considering the thermodynamic and environmental properties. Besides the working fluid and operating parameters, adoption of proper cycle forms can also enhance an ORC capability to recover low-grade heat. Mago *et al.* [11] assessed the performances of the basic and the regenerative ORC both using dry fluids. Heberle *et al.* [12] evaluated a combined heat and power generation which improved the exergy efficiency markedly for the geothermal resource utilization. Attempts are also made to find suitable working fluids for specific applications [13-15]. The performances of ORC for low-grade heat recovery, however, have not been illuminated in the cases of using various types of organic fluids under a certain expansion.

The purpose of this study is to explore the performances of ORC under saturated expansions using organic dry/isentropic fluids, and under superheated expansions using organic wet fluids. The organic fluids are chosen by considering their critical temperature without regarding of their environmental property in order to make them almost evenly distributed in the studied boundary of critical temperature. Relationships between performance parameters and critical temperatures are established based on inlet temperature, mass flow rate, and specific heat capacity of hot fluid in a specific working condition, and are verified later at varied evaporation temperatures and inlet temperatures of hot fluid.

Thermodynamic analysis of organic Rankine cycle

Basic processes of ORC and working fluid

A typical ORC for low-grade heat recovery consists of a pump, an evaporator, an expander, and a condenser, as shown in fig. 1. The cycle is divided into pumping (1-2), constant-pressure heat addition (2-3), expansion (3-4), and constant-pressure heat rejection (4-1) processes. After it becomes saturated liquid through the condenser, the working fluid is pumped into the evaporator where it gains heat from the hot fluid and finally turns into saturated or superheated vapor.

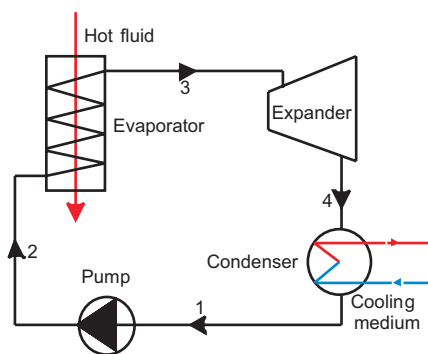


Figure 1. Schematic diagram of organic Rankine cycle

The vapor expands in the expander and thus power is generated. The exit fluid from the expander flows into the condenser and is cooled to saturated liquid again. The working fluid is circulated in an ORC *via* these processes. In this study we assume the ORC is in a steady-state. There are no pressure drops in the evaporator, the condenser, and the pipes, and no heat loss in all components.

As shown in fig. 2, organic fluids, in terms of the temperature-entropy diagrams, are commonly classified as dry, isentropic, and wet fluid, which has a positive, infinite, and negative slope in saturated vapor curve, respectively. When a wet fluid flows in expander as saturated vapor or becomes saturated vapor at the outlet of expander after actual expansion, the fluid inside the expander may form droplets, which results in erosion of the expander blades. Therefore, the wet fluid at the inlet of an expander has to be superheated enough. Due to the lower heat transfer coefficient in the vapor phase, the heat transfer area required for superheating should be larger and the cost of ORC

increases as compared with saturated expansions. For wet fluids, the degree of superheat should be set as small as possible, and it is applicable if the fluid becomes saturated vapor after isentropic expansion in the expander, as shown in fig. 2(c). As for dry and isentropic fluids, there is no need for superheating and they normally expand under the saturated vapor state. Hence, in this study we categorize the expansions of the organic working fluids as two types: (a) saturated expansion of dry/isentropic fluids, and (b) superheated expansion of wet fluids.

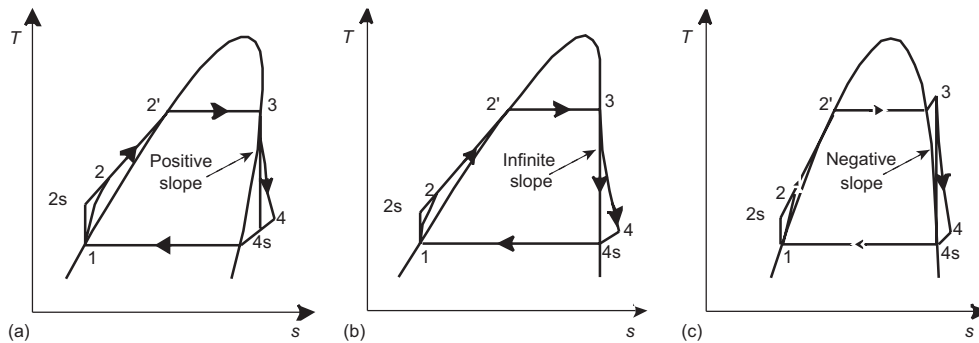


Figure 2. Temperature-entropy diagram of ORC; (a) dry fluid, (b) isentropic fluid, and (c) wet fluid

Heat exchange in the evaporator

The temperature variation between the hot fluid and the working fluid in the evaporator of an ORC is shown in fig. 3. The sub-cooled fluid from the pump at temperature T_2 absorbs heat from the hot fluid and becomes saturated liquid, and at that point the temperature difference ΔT between the hot fluid and the working fluid is minimum. The saturated liquid is vaporized by the heat gain from the hot fluid, and is turned into saturated vapor at temperature T_e . The saturated vapor of a dry/isentropic fluid flows out of the evaporator and enters the expander, fig. 3(a); however, the saturated vapor of a wet fluid is superheated to temperature T_3 before it enters the expander, fig. 3(b). During the above heat exchange, the temperature of the hot fluid decreases from T_{in} to T_{out} . The specific heat capacity c_p of the hot fluid at constant pressure is assumed to be constant.

Applying the principle of energy conservation to the heat transfer process in the evaporator, we obtain:

$$\dot{m}_{hf} c_p \Delta T_a = \dot{m}_{wf} (h_{2'} - h_2) \quad (1)$$

$$\dot{m}_{hf} c_p \Delta T_b = \dot{m}_{wf} (h_3 - h_{2'}) \quad (2)$$

$$\dot{m}_{hf} c_p (T_{in} - T_{out}) = \dot{m}_{wf} (h_3 - h_2) \quad (3)$$

where \dot{m}_{hf} and \dot{m}_{wf} are the mass flow rates of the hot fluid and of the working fluid, ΔT_a and ΔT_b are the temperature drops of the hot fluid in the subcooled and vaporizing sections, h_2 and h_3 are the specific enthalpies of the working fluid at the pump's outlet and at the expander's inlet, and $h_{2'}$ is the specific enthalpy of the working fluid in saturated liquid state at evaporation temperature.

According to the geometric relationship in fig. 3, ΔT_a and ΔT_b satisfy:

$$\frac{\Delta T_b}{\Delta T_a} = \frac{T_e + \Delta T - T_{out}}{T_{in} - \Delta T - T_e} \quad (4)$$

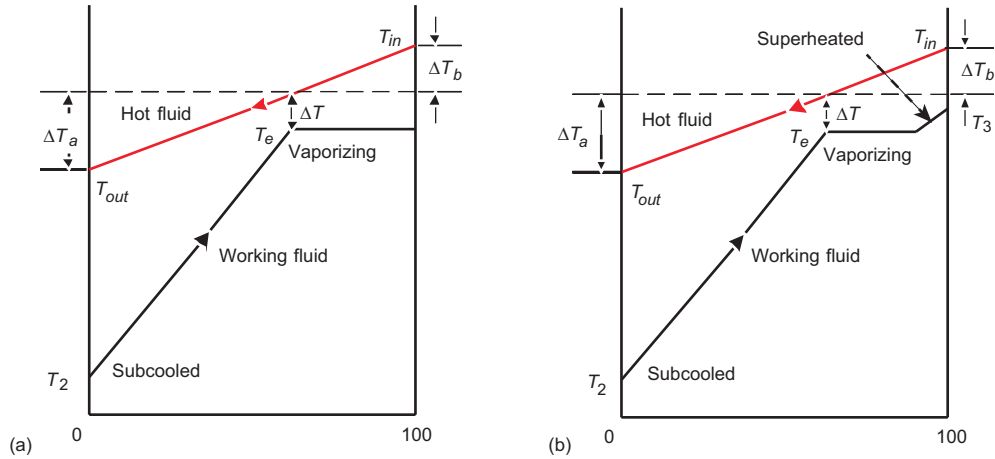


Figure 3. Temperature variation between hot fluid and working fluid in the evaporator; (a) dry/isentropic fluid and (b) wet fluid

Substitute eqs. (1) and (2) into eq. (4), we obtain:

$$T_{out} = T_e + \Delta T - (T_{in} - T_e - \Delta T) \frac{h_{2'} - h_2}{h_3 - h_2} \quad (5)$$

Combine eqs. (3) and (5), we get:

$$\dot{m}_{wf} = \frac{\dot{m}_{hf} c_p (T_{in} - T_e - \Delta T)}{h_3 - h_2} \quad (6)$$

Evaluation of performance parameters

The ORC system discussed in this paper is steady and non-reaction [16]. We assume the cooling medium temperature T_L does not change during the condensation process and the ambient temperature is T_0 .

In the pumping process, the power consumed is:

$$W_p = \frac{W_{p,ideal}}{\eta_p} = \frac{\dot{m}_{wf} (h_{2s} - h_1)}{\eta_p} \quad (7)$$

where W_p and $W_{p,ideal}$ are the actual and ideal power consumptions of the pump, η_p is the isentropic efficiency of the pump, and h_1 and h_{2s} are the specific enthalpies of the working fluid at the inlet and the outlet of the pump in ideal cases.

The irreversibility rate in the pumping process is:

$$\dot{I}_p = T_0 \dot{m}_{wf} (s_2 - s_1) \quad (8)$$

where s_1 and s_2 are the specific entropies of the working fluid at the inlet and the outlet of the pump.

In the constant-pressure heat addition process, the heat absorbed by the working fluid is:

$$\dot{Q}_e = \dot{m}_{wf}(h_3 - h_2) \quad (9)$$

The irreversibility rate in the evaporator is:

$$\dot{I}_e = T_0 \dot{m}_{wf} \left[(s_3 - s_2) - \frac{2(h_3 - h_2)}{T_{in} + T_{out}} \right] \quad (10)$$

where s_3 is the specific entropy of the working fluid at the outlet of the evaporator.

In the expansion process, the power generated by the expander is:

$$W_t = W_{t,ideal} \eta_t = \dot{m}_{wf}(h_3 - h_{4s}) \eta_t \quad (11)$$

where W_t and $W_{t,ideal}$ are the actual and ideal powers generated by the expander, η_t is the isentropic efficiency of the expander, and h_{4s} – the specific enthalpy of the working fluid at the expander outlet in ideal cases.

The irreversibility rate in expansion is:

$$\dot{I}_t = T_0 \dot{m}_{wf}(s_4 - s_3) \quad (12)$$

where s_4 is the specific entropy of the working fluid at the expander's outlet.

In the constant-pressure heat rejection process, the heat transferred in the condenser is:

$$\dot{Q}_c = \dot{m}_{wf}(h_1 - h_4) \quad (13)$$

where h_4 is the specific enthalpy of the working fluid at the expander's outlet.

The irreversibility rate in the condenser is:

$$\dot{I}_c = T_0 \dot{m}_{wf} \left[(s_1 - s_4) - \frac{h_1 - h_4}{T_L} \right] \quad (14)$$

The net power, the difference between the power generated by the expander and the power consumed by the pump, is calculated by:

$$W_{net} = \dot{m}_{wf} \left[(h_3 - h_{4s}) \eta_t - \frac{h_{2s} - h_1}{\eta_p} \right] \quad (15)$$

The thermal efficiency defined as the ratio of the net power to the heat absorbed by the working fluid in the evaporator, can be expressed as:

$$\eta_{cycle} = \frac{(h_3 - h_{4s}) \eta_t + (h_1 - h_{2s}) \eta_p^{-1}}{h_3 - h_2} \quad (16)$$

The exergy efficiency is:

$$\eta_{exergy} = \left(\frac{(h_3 - h_{4s}) \eta_t + (h_1 - h_{2s}) \eta_p^{-1}}{h_3 - h_2} \right) \left(1 - \frac{2T_L}{T_{in} + T_{out}} \right)^{-1} \quad (17)$$

By summing eqs. (8), (10), (12), and (14), we obtain the total cycle irreversibility rate:

$$\dot{I}_{\text{cycle}} = \dot{m}_{\text{wf}} T_0 \left[-\frac{2(h_3 - h_2)}{T_{\text{in}} + T_{\text{out}}} - \frac{h_1 - h_4}{T_L} \right] \quad (18)$$

The total heat-recovery efficiency [7], defined as the ratio of the net power to the available energy in ideal case, is computed by:

$$\eta_T = \frac{T_{\text{in}} - T_{\text{out}}}{T_{\text{in}} - T_0} \cdot \eta_{\text{cycle}} \quad (19)$$

Table 1. Thermophysical properties of working fluids

Working fluid	Fluid type	Molecular mass [g mol^{-1}]	T_c [K]	p_c [MPa]
R227ea	dry	170.03	375.8	3.00
RC318	dry	200.03	388.2	2.78
R600a	dry	58.12	407.7	3.63
R114	dry	170.92	418.7	3.26
R600	dry	58.12	425.0	3.80
R245fa	dry	134.05	427.0	3.65
R245ca	dry	134.05	447.4	3.93
R123	dry	152.93	456.7	3.66
R141b	isotropic	116.95	477.4	4.21
R113	dry	187.38	487.1	3.39
R125	wet	102.02	339.0	3.62
R143a	wet	84.04	345.7	3.76
R32	wet	52.02	351.1	5.78
R22	wet	86.47	369.1	4.99
R290	wet	44.10	369.7	4.25
R134a	wet	102.03	374.1	4.06
R12	wet	120.91	385.0	4.14
R152a	wet	66.05	386.3	4.52
R142b	wet	100.5	410.1	4.06

Results and discussion

To study the dependence of the performance parameters on the critical temperature of the working fluid under a saturated or superheated expansion, we selected ten organic dry/isentropic fluids with the critical temperatures from 375.8 to 487.1 K, and nine organic wet fluids with the critical temperatures from 339 to 410.1 K. The critical temperature scopes of the refrigerants in Refprop 6.01 software are 375.8 to 487.1 K for dry/isentropic fluids and 339.0 to 410.1 K for wet fluids. The 19 fluids selected satisfy the criteria that their critical temperatures are evenly distributed across the scopes of the critical temperatures studied. The fluids and their thermophysical properties [17] are listed in tab. 1. In the following analyses, we assumed that the isentropic efficiency η_p of the pump was 85%, the isentropic efficiency η_t of the expander was 80%, the mass flow rate \dot{m}_{hf} of the hot fluid was 1 kg/s, the specific heat capacity c_p of the hot fluid at

constant pressure was 1 kJ/kgK, the minimum temperature difference ΔT in the evaporator was 10 K, and the condensation temperature of working fluid T_{con} , the cooling medium temperature T_L , and the ambient temperature T_0 are 293 K, 283 K, and 288 K, respectively.

Saturated expansion of dry/isentropic fluids

Performance in a specific condition

For all ORC using dry/isentropic fluids in the study, we set the evaporation temperature as 353 K, and the inlet temperature of the hot fluid as 373 K. Choosing 373 K as the temperature of the hot fluid is normal in the utilization of low-temperature heat sources, such as solar and geothermal energy. It is rational to adopt 353 K as the evaporation temperature to limit the ORC being a subcritical cycle and to maintain appropriate temperature difference be-

tween the hot fluid and the working fluid in the evaporator. The performance parameters of the ORC using the dry/isentropic fluids in tab. 1 are calculated by the expressions in the section *Evaluation of performance parameters*. The exergy efficiency is not presented, because it has the same variation as the thermal efficiency at constant condensation temperature and inlet temperature of hot fluid.

Figure 4 illustrates the dependence of the ORC performance parameters on the critical temperatures of the dry/isentropic fluids. The evaporation and condensing pressures, the net power, the total cycle irreversibility rate, and the total heat-recovery efficiency decrease with the critical temperature. On the contrary, the outlet temperature of the hot fluid and the thermal efficiency increase with the critical temperature.

It is seen in fig. 4(b) that the minimum condensing pressure is 0.0367 MPa (less than atmospheric pressure), meaning that using the dry/isentropic fluid with a high critical temperature may cause vacuum in the system and raise the risk of air entering. As shown in fig. 4(d) and 4(e), the net power decreases whereas the thermal efficiency increases with the critical temperature. The reason for this phenomenon is that the ratio between the decreases of the net power and of the heat absorbed caused by the selection of a higher critical-temperature working fluid is smaller than the thermal efficiency by using the working fluid with a lower critical temperature. The maximum net power and thermal efficiency are 2.101 kW and 11.6%, which are achieved by using R227ea and R141b, respectively. By examining fig. 4(d) and 4(g), we find a considerable similarity in the variation of the total heat-recovery efficiency and the net power with the critical temperature.

Performance at varied evaporation temperatures

The evaporation temperature has an important impact on the performance of an ORC. We discuss the ORC performance parameters at various evaporation temperatures in this section. The evaporation temperature was increased from 303 to 358 K with a 5 K step. The inlet temperature of the hot fluid was assumed to be 373 K all the same. The dry/isentropic fluids studied were R227ea, R600, and R113, due to their large differences in the critical temperatures. Since the condensation temperature was constant, the condensing pressure did not change for any specific fluid regardless of the variation of the evaporation temperature. Consequently, it does not need to analyze the condensing pressure. Figure 5 presents the relationships of the evaporation pressure, the outlet temperature of the hot fluid, the

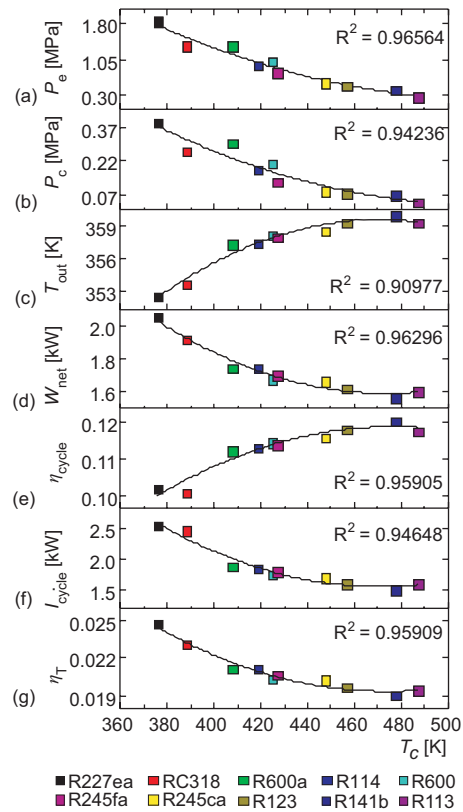


Figure 4. Performance parameters vs. critical temperatures for dry/isentropic fluids; (a) evaporation pressure, (b) condensing pressure, (c) outlet temperature of hot fluid, (d) net power, (e) thermal efficiency, (f) total cycle irreversibility rate, and (g) total heat-recovery efficiency

total heat-recovery efficiency and the net power with the critical temperature.

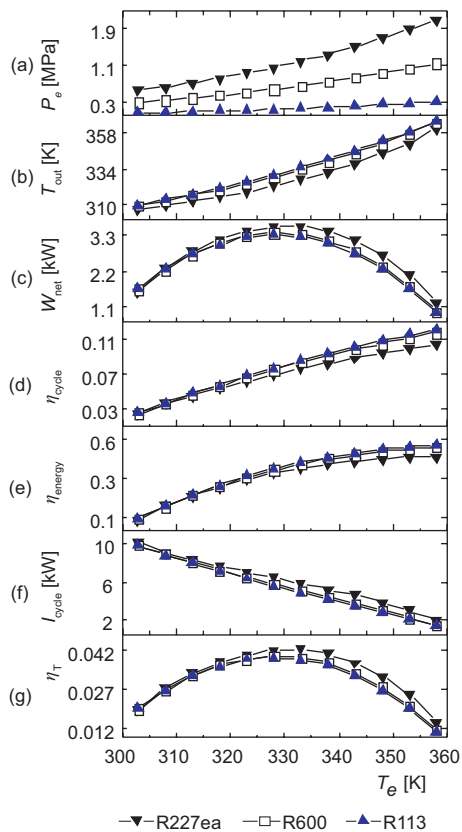


Figure 5. Performance parameters vs. evaporation temperatures for dry/isentropic fluids; (a) evaporation pressure, (b) outlet temperature of hot fluid, (c) net power, (d) thermal efficiency, (e) total cycle irreversibility rate, and (f) total heat-recovery efficiency

net power, the thermal efficiency, the exergy efficiency, the total cycle irreversibility rate, and the total heat-recovery efficiency with the evaporation temperature for the dry/isentropic fluids R227ea, R600, and R113.

Figure 5 shows the curves of the evaporation pressure, the outlet temperature of the hot fluid, the net power, the thermal efficiency, the exergy efficiency, the total cycle irreversibility rate, and the total heat-recovery efficiency vs. the evaporation temperature do not intersect, which implies that the evaporation temperature has little effect on the relationships between these performance parameters and the critical temperatures of the dry/isentropic fluids studied. The evaporation pressure, the outlet temperature of the hot fluid, the thermal efficiency, and the exergy efficiency increase with the evaporation temperature; however, the total cycle irreversibility rate decreases with the evaporation temperature. The net power and the total heat-recovery efficiency are both parabolic-like functions of the evaporation temperature with identical variation trend.

With the increase of evaporation temperature, the temperature of the hot fluid also increases at the status where the temperature difference between the working fluid and the hot fluid is minimum (10 K), as shown in fig. 3(a). Its increment is equal to that of the evaporation temperature. But the increased sensible heat of the hot fluid is greater than that of the liquid working fluid caused by the increase of the evaporation temperature, so the outlet temperature of the hot fluid increases as shown in fig. 5(b).

As shown in fig. 5(c), excessively high evaporation temperature may reduce the net power. The reason is that although the net power generated by the working fluid of unit mass flow increases with the increasing of the evaporation temperature, the mass flow rate of the working fluid reversely decreases with the evaporation temperature increases under a constant flow rate of hot fluid. The effect from the decrease of the hot fluid on the net power is primary at the high evaporation temperature. As for R227ea, the maximum net power 3.583 kW is achieved at the evaporation temperature 333 K, but the net power decreases with the evaporation temperature afterwards. As for R600 and R113, the evaporation temperatures for the maximum net powers are both 328 K. Therefore, the net power as well as the thermal efficiency should be taken into account to determine a suitable evaporation temperature.

The thermal efficiency increases markedly when the net power and the outlet temperature of the hot fluid both increase. As the net power decreases, the thermal efficiency still increases as shown in fig. 5(d), which indicates the effect of the increase of the evaporation

temperature on the decrease of the heat absorbed by the working fluid is greater than that on the decrease of the net power. Figure 5(e) and eq. (17) illustrate that the exergy efficiency is mainly determined by the thermal efficiency, and the increase of the outlet temperature of the hot fluid has a little effect on the decrease of the exergy efficiency. Equation (19) and fig. 5(g) indicate that the effect of the outlet temperature of the hot fluid increase on the total heat-recovery efficiency is greater than the increase of thermal efficiency on total heat-recovery efficiency as the evaporation temperature is low. However, when the evaporation temperature increases to a higher value, the total heat-recovery efficiency appears to decrease.

Performance at varied inlet temperatures of hot fluid

In this section, we evaluate the ORC performance parameters at varied inlet temperatures of the hot fluid which ranged from 368 K to 423 K with a 5 K step. The evaporation temperature was assumed to be 353 K. The dry/isentropic fluids studied were R227ea, R600, and R113. Since the evaporation temperature and the condensation temperature were constant, the evaporation pressure, the condensing pressure, and the thermal efficiency did not change with the inlet temperatures of the hot fluid, which means the three performance parameters mentioned do not need to be discussed.

Figure 6 illustrates that the inlet temperature of the hot fluid also hardly affects the relationships between the performance parameters, except the exergy efficiency and the critical temperatures of the dry/isentropic fluids studied, because only the curves in fig. 6(c) intersect. The outlet temperature of the hot fluid decreases with the inlet temperature of the hot fluid. On the contrary, the net power, the total cycle irreversibility rate, and the total heat-recovery efficiency increase with the inlet temperature of the hot fluid.

Equation (5) indicates the outlet temperature of the hot fluid is a linear function of its inlet temperature, provided that the evaporation temperature, the condensing temperature, and the isentropic efficiency of the expander keep unchanged, as shown in fig. 6(a). At the varied inlet temperature of the hot fluid, the net power is a linear function of the mass flow rate of the working fluid that is proportional to the inlet temperature of the hot fluid, which can be seen from eqs. (15) and (6).

Figures 6(b) and (e) show that the variation trend of the total heat-recovery efficiency differs from that of the net power, which is unlike the cases at varied evaporation temperatures. At the inlet temperature of the hot fluid between 368 and 423 K, the net power of the ORC using R227ea increases from 1.051 kW to 12.609 kW, fig. 6(b), whereas the exergy efficiency of the ORC using R113 decreases from 51.92% to 45.35%, fig. 6(c). The exergy efficiency decreases monotonically due to the continual increment of the inlet temperature of the hot fluid and the invariability of the thermal effi-

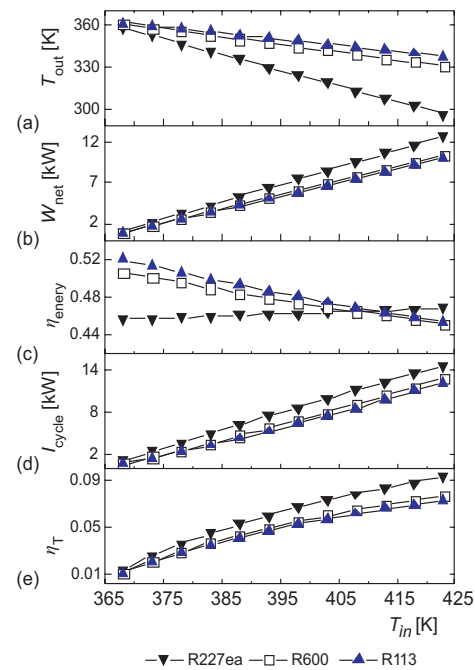


Figure 6. Performance parameters vs. inlet temperatures of the hot fluid for dry/isentropic fluids; (a) outlet temperature of hot fluid, (b) net power, (c) the exergy efficiency, (d) total cycle irreversibility rate, and (e) total heat-recovery efficiency

ciency as adopting R600 and R113. As for R227ea, the decrease of the outlet temperature of the hot fluid is too large and makes the exergy efficiency inversely increase, which can be interpreted by eqs. (16) and (17). As shown in fig. 6(e), the total heat-recovery efficiency increases because the thermal efficiency is a constant and the increment of the numerator is greater than that of the denominator for the left expression of the right side of eq. (19).

Superheated expansion of wet fluids

The degree of superheat evaporation temperature only depends on the evaporation temperature, because the wet fluids become saturated vapor after isentropic expansion in ex-

pander and the condensation temperature does not change. The states of the wet fluids after expansion in expander are all superheated.

Performance in a specific condition

The performance parameters using the wet fluids in tab. 1 are shown in fig. 7 when the evaporation temperature was 323 K and the inlet temperature of the hot fluid was 363 K. The total heat-recovery efficiency is not presented because of its identical variation trend resembling the net power like the cases using the dry/isentropic fluids.

The variations of the parameters of the ORC using wet fluids presented in fig. 7 are nearly identical to those using dry/isentropic fluids, as shown in figs. 4, 7(a), and 7(b) show that the evaporation and the condensing pressures are both linear function of the critical temperature of the wet fluid, which is different from the dry/isentropic fluids. Moreover, the values of the other performance parameters for wet fluids are more dispersive than those for dry/isentropic fluids, as shown in figs. 7(c)-(g). This phenomenon is caused by the temperature difference of the working fluid superheated at the inlet of the expander when using different wet fluids. As a whole, with the increase of the critical temperatures of the wet fluids, the evaporation and condensing pressures, the net power, and the total heat-recovery efficiency decrease, whereas the outlet temperature of the hot fluid, the thermal efficiency, and the exergy efficiency increase.

The lowest condensing pressure is 0.288 MPa (R142b), which is greater than the atmospheric pressure. Consequently, ORC using wet fluids do not need to care about the vacuum produced in the operation process, but the large evaporation pressure may raise the investment cost

such as the adoption of high strength steels. The highest and the lowest net power in the ORC using the nine wet fluids are 2.770 kW (R125) and 2.426 kW (R142b). The ORC using R32 has

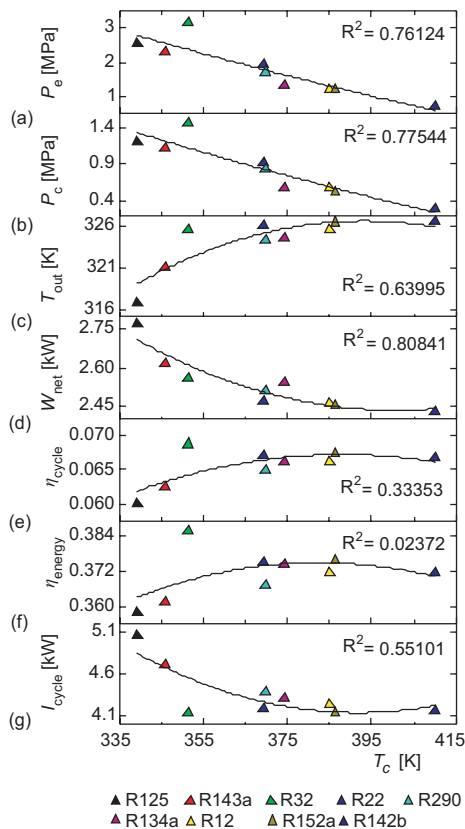


Figure 7. Performance parameters vs. critical temperatures for wet fluids; (a) evaporation pressure, (b) condensing pressure, (c) outlet temperature of hot fluid, (d) net power, (e) thermal efficiency, (f) the exergy efficiency, and (g) total cycle irreversibility rate

the maximum thermal efficiency (6.88%), the maximum exergy efficiency (38.56%), and the minimum total cycle irreversibility rate (4.146 kW), which indicates the superiority of R32.

Performance at varied evaporation temperatures

Figure 8 shows the performance parameters using selected wet fluids at varied evaporation temperatures ranging from 298 to 338 K with a 5 K step. These wet fluids were R125, R290, and R142b. The inlet temperature of the hot fluid was 363 K. The variation of the evaporation pressures using wet fluids is similar to those using dry/isentropic fluids, as shown in fig. 5(a). In view of the similarity of the variation between the net power and the total heat-recovery efficiency with the evaporation temperature, the evaporation pressure and the total heat-recovery efficiency are omitted in fig. 8.

The appearance of the intersection points in figs. 8(b)-(e) illustrates that the evaporation temperature has a little effect on the relationships between these performance parameters and the critical temperatures of the wet fluids studied. Compared to dry/isentropic fluids, it is mainly caused by the difference of the temperature of the working fluid superheated at the inlet of the expander for various wet fluids. The temperatures superheated increase from 0.3, 1.8, and 0.3 K to 6.1, 4.1, and 1.3 K for R125, R290, and R142b, respectively. The temperature superheated of R125 is considerably large compared to that of R290 and R142b, so the performance parameters in figs. 8(b)-(e) increase or decrease sharply with the evaporation temperature increases for R125. Therefore, the curves in fig. 8 intersect.

Figure 8 illustrates that the outlet temperature of the hot fluid, the thermal efficiency, and the exergy efficiency increase with the evaporation temperature, whereas the total cycle irreversibility rate decreases. Differently, the net power of R125 increases basically with the evaporation temperature from 298 to 338 K; however, the net powers of R290 and R142b increase first and decrease afterwards, and their maximum values are, respectively, 2.509 and 2.426 kW achieved both at the evaporation temperature 323 K. The anomaly of the net power of R125 is mainly caused by the small difference between the critical temperature (339 K) of R125 and the evaporation temperature, in which conditions the ORC approach to the transcritical state. Moreover, the curves of the net powers intersect with each other as the evaporation temperature increases and the same situation appears in the thermal efficiency, the exergy efficiency, and the total cycle irreversibility rate, which means that the evaporation temperature may affect the relative distribution of these performance parameters vs. the critical temperatures. For instance, when the evaporation temperature is below 306 K, the tendency of the net power is R290 > R125 > R142b; above that evaporation temperature, the tendency changes to R125 > R290 > R142b.

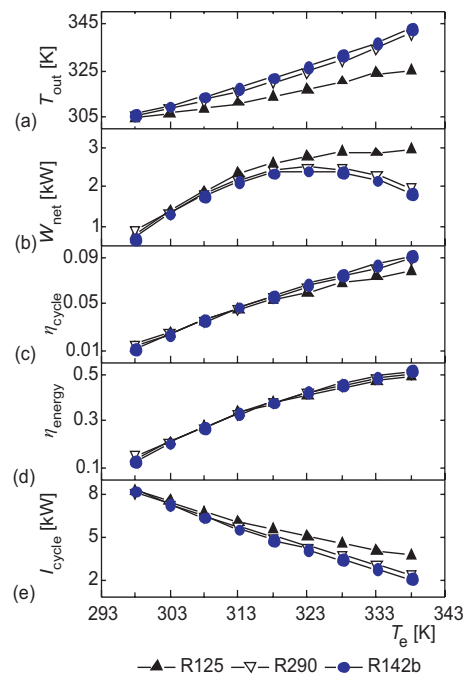


Figure 8. Performance parameters vs. evaporation temperatures for wet fluids; (a) outlet temperature of hot fluid, (b) net power, (c) thermal efficiency, (d) the exergy efficiency, and (e) total cycle irreversibility rate

Performance at varied inlet temperatures of hot fluid

The variations of the performance parameters of ORC using wet fluids at various inlet temperatures of the hot fluid from 348 to 393 K with a 5 K step were also obtained. The evaporation temperature was assumed to be 328 K, and the wet fluids studied were R125, R290, and R142b. The analysis process is the same as the section *Performance at varied inlet temperatures of hot fluid*. The results reveal that the variation trends of the performance parameters of the ORC using the wet fluids are identical to those of using dry/isentropic fluids, which have been discussed in detail in the same section.

Conclusions

In this paper, the performances of ORC using different types of organic fluids were analyzed. The relationships between the ORC performance parameters and the critical temperatures of organic fluids are established in a specific working condition, and are verified at varied evaporation temperatures and inlet temperatures of the hot fluid.

Under saturated expansions, the thermal efficiency, the exergy efficiency, and the outlet temperature of the hot fluid increase with the critical temperatures of the dry/isentropic fluids; however, the evaporation and condensing pressures, the net power, the total cycle irreversibility rate, and the total heat-recovery efficiency decrease with the critical temperatures. For the superheated expansions of the wet fluids, the relationships between the performance parameters and the critical temperatures seem a bit irregular in comparison with the saturated expansions of the dry/isentropic fluids. The evaporation temperature may affect the relative distribution of the performance parameters of the ORC using different wet fluids except the outlet temperature of the hot fluid, the evaporation and condensing pressure. The inlet temperature of the hot fluid has an impact on the relative distribution of the exergy efficiency for all types of organic fluids.

To achieve a high net power, the organic fluids with the small difference between its critical temperature and the inlet temperature of the hot fluid are recommended. Thus the scope of candidate organic fluids for a specific thermal source can be narrowed considerably, which facilitates the process of working fluid selection. However, comparisons between the saturated expansion of dry/isentropic fluids and the superheated expansion of wet fluids still remain open for further investigations, due to the difficulty in seeking enough groups of dry/isentropic fluids and wet fluids with nearly the same critical temperatures.

Acknowledgments

This work is supported by the National Natural Science Foundation of China (Grant Nos. U0937604, 50876116), the Hunan Scientific Program (Grant No. 2011FJ3246), and the Fundamental Research Funds for the Central Universities of China (Grant No. 2010QZZD0107).

References

- [1] Larjola, J., Electricity from Industrial Waste Heat Using High-Speed Organic Rankine Cycle (ORC), *International Journal of Production Economics*, 41 (1995), 1-3, pp. 227-235
- [2] Hung, T. C., et al., A Review of Organic Rankine Cycles (ORCs) for the Recovery of Low-Grade Waste Heat, *Energy*, 22 (1997), 7, pp. 661-667
- [3] Wei, L., et al., Efficiency Improving Strategies of Low-Temperature Heat Conversion Systems Using Organic Rankine Cycles: an Overview, *Energy Sources Part a-Recovery Utilization and Environmental Effects*, 33 (2011), 9, pp. 869-878

- [4] Schuster, A., et al., Efficiency Optimization Potential in Supercritical Organic Rankine Cycles, *Energy*, 35 (2010), 2, pp. 1033-1039
- [5] Guo, T., et al., Comparative Analysis of CO₂-Based Transcritical Rankine Cycle and HFC245fa-Based Subcritical Organic Rankine Cycle Using Low-Temperature Geothermal Source, *Science China-Technological Sciences*, 53 (2010), 6, pp. 1638-1646
- [6] Guo, T., et al., Comparative Analysis of Natural and Conventional Working Fluids for Use in Transcritical Rankine Cycle Using Low-Temperature Geothermal Source, *International Journal of Energy Research*, 35 (2011), 6, pp. 530-544
- [7] Liu, B. T., et al., Effect of Working Fluids on Organic Rankine Cycle for Waste Heat Recovery, *Energy*, 29 (2004), 8, pp. 1207-1217
- [8] Wei, D. H., et al., Performance Analysis and Optimization of Organic Rankine Cycle (ORC) for Waste Heat Recovery, *Energy Conversion and Management*, 48 (2007), 4, pp. 1113-1119
- [9] Etemoglu, A. B., Thermodynamic Evaluation of Geothermal Power Generation Systems in Turkey, *Energy Sources Part a-Recovery Utilization and Environmental Effects*, 30 (2008), 10, pp. 905-916
- [10] Tchanche, B. F., et al., Fluid Selection for a Low-Temperature Solar Organic Rankine Cycle, *Applied Thermal Engineering*, 29 (2009), 11-12, pp. 2468-2476
- [11] Mago, P. J., et al., An Examination of Regenerative Organic Rankine Cycles Using Dry Fluids, *Applied Thermal Engineering*, 28 (2008), 8-9, pp. 998-1007
- [12] Heberle, F., Bruggemann, D., Exergy Based Fluid Selection for a Geothermal Organic Rankine Cycle for Combined Heat and Power Generation, *Applied Thermal Engineering*, 30 (2010), 11-12, pp. 1326-1332
- [13] Al-Sulaiman, F. A., et al., Energy Analysis of a Trigeration Plant Based on Solid Oxide Fuel Cell and Organic Rankine Cycle, *International Journal of Hydrogen Energy*, 35 (2010), 10, pp. 5104-5113
- [14] Borsukiewicz-Gozdur, A., Nowak, W., Feasibility Study and Energy Efficiency Estimation of Geothermal Power Station Based on Medium Enthalpy Water, *Thermal Science*, 11 (2007), 3, pp. 135-142
- [15] Moro, R., et al., ORC Technology for Waste-Wood to Energy Conversion in the Furniture Manufacturing Industry, *Thermal Science*, 12 (2008), 4, pp. 61-73
- [16] DiPippo, R., Second Law Assessment of Binary Plants Generating Power from Low-Temperature Geothermal Fluids, *Geothermics*, 33 (2004), 5, pp. 565-586
- [17] Calm, J. M., Hourahan, G. C., Refrigerant Data Update, *Heating/Piping/Air Conditioning Engineering*, 79 (2007), 1, pp. 50-64